ACS OMEGA

http://pubs.acs.org/journal/acsodf

Mini-Review

# Alternative Approaches to Understand Microtubule Cap Morphology and Function

María Ángela Oliva, Federico Gago, Shinji Kamimura, and J. Fernando Díaz*

Cite This: *ACS Omega* 2023, 8, 3540−3550

Read Online

ACCESS | Metrics & More | Article Recommendations

**ABSTRACT:** Microtubules (MTs) are essential cellular machines built from concatenated $\alpha\beta$-tubulin heterodimers. They are responsible for two central and opposite functions from the dynamic point of view: scaffolding (static filaments) and force generation (dynamic MTs). These roles engage multiple physiological processes, including cell shape, polarization, division and movement, and intracellular long-distance transport. At the most basic level, the MT regulation is chemical because GTP binding and hydrolysis have the ability to promote assembly and disassembly in the absence of any other constraint. Due to the stochastic GTP hydrolysis, a chemical gradient from GTP-bound to GDP-bound tubulin is created at the MT growing end (GTP cap), which is translated into a cascade of structural regulatory changes known as MT maturation. This is an area of intense research, and several models have been proposed based on information mostly gathered from macromolecular crystallography and cryo-electron microscopy studies. However, these classical structural biology methods lack temporal resolution and can be complemented, as shown in this mini-review, by other approaches such as time-resolved fiber diffraction and computational modeling. Together with studies on structurally similar tubulins from the prokaryotic world, these inputs can provide novel insights on MT assembly, dynamics, and the GTP cap.

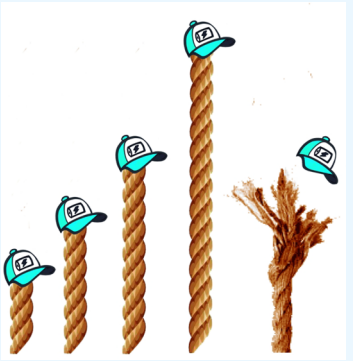

## INTRODUCTION

The essential role of MTs in the cell division and vascularization process made these cellular structures an obvious target in the treatment of cancer. In addition, their implication in intracellular long-distance transport and scaffolding is behind the pharmacological regulation of MTs in inflammation and neurodegeneration. There is a plethora of MT-regulating compounds that bind to up to eight different pharmacological pockets in tubulin[1−3] and either activate or turn off the tubulin molecule, hence perturbing MT function through stabilization or disassembly. Often, MT stabilizing agents (MSAs) promote assembly and settle the structure of these filaments through the axial and/or the lateral contacts, whereas destabilizers (MDAs) prevent (curved-to-straight) conformational changes upon assembly or block the axial molecular interacting surfaces, thus preventing the formation of MTs. However, the precise structural mechanisms underlying the pharmacological regulation of tubulin are, in some cases, not well known yet, and this hampers the rational fine-tuning of MT function in those diseases without inducing further alterations conducive to side effects during treatments.

The spatial and temporal control of MT assembly and dynamics is finely tuned through a complex regulatory system that relies both on tubulin itself (isotype production and posttranslational modifications) and on an interacting network of partner proteins. At the simplest level, tubulin is a molecular switch regulated by guanine nucleotides. GTP binding induces an assembly-prone conformation (i.e., tubulin activation), while in the GDP-bound state tubulin is deactivated. MTs are nanomachines that grow from the successive addition of GTP-bound $\alpha\beta$-tubulin heterodimers to the tips and shrink through the loss of GDP-tubulin molecules from the tips. Since the GTP-binding site and the crucial catalytic residue ($\alpha$E254) are in opposite regions of the tubulin molecule, MT assembly is required for the completion of the catalytic site, both by the obvious need of longitudinal contacts and through a curved-to-straight conformational change in tubulin, resulting from the formation of lateral contacts.[4] The combination of noncoupled stochastic GTP hydrolysis in $\beta$-tubulin and the progressive incorporation of tubulin molecules at the tip creates a chemical gradient because GTP-tubulin evolves to form the intermediate GDP·$P_i$-tubulin and finally GDP-tubulin (in the core of MTs), in what is known as a tip maturation process.[5,6] Remarkably, this chemical gradient constitutes the central point of the cellular MT regulation by MT-associated proteins (MAPs) because these specifically recognize structural states derived from the chemical signals at the MT ends.[7,8] Many MAPs bind to certain areas on MTs and modulate their

Received: October 27, 2022
Accepted: December 26, 2022
Published: January 13, 2023





https://doi.org/10.1021/acsomega.2c06926
*ACS Omega* 2023, 8, 3540−3550

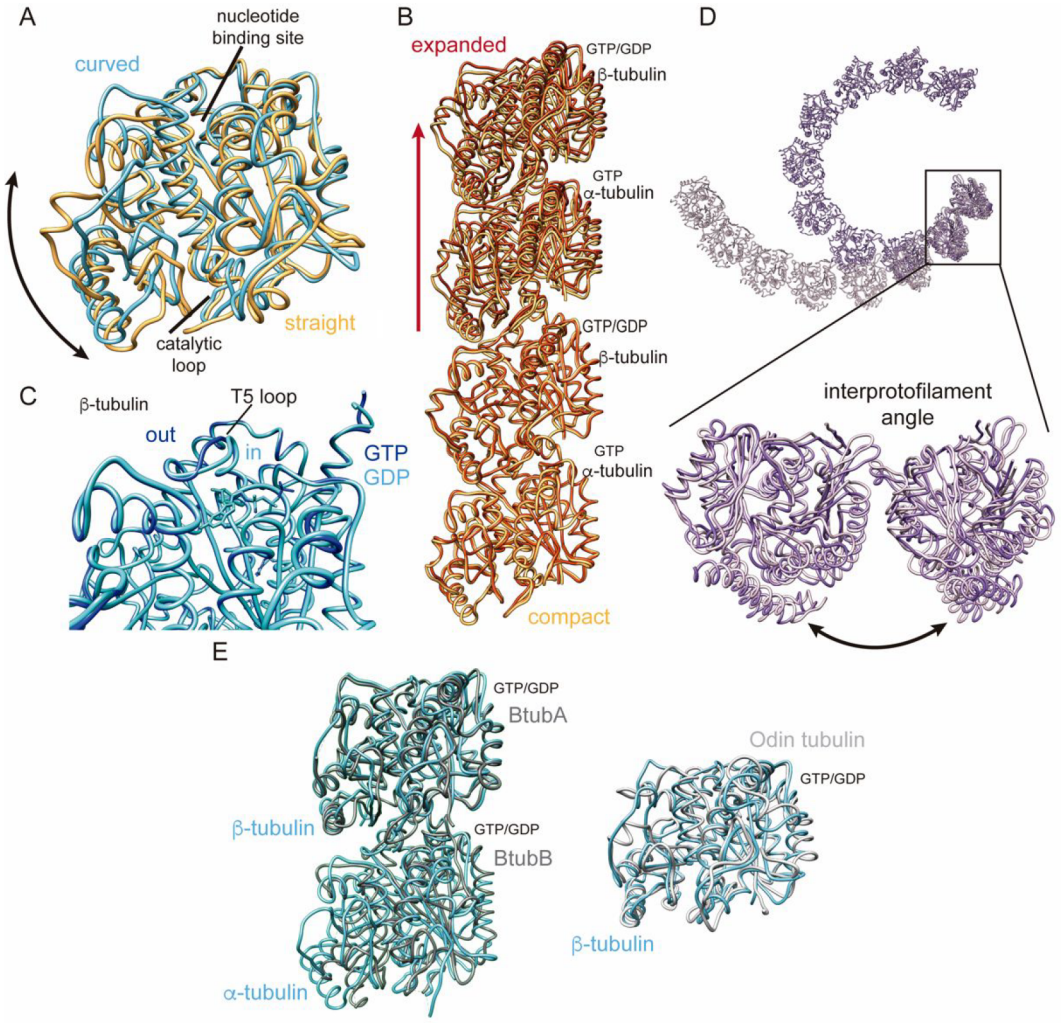


**Figure 1.** (A–D) Scheme of the main conformational changes in tubulin and MTs.[13,14,16,25] (E) Prokaryotic tubulins described in the manuscript.[23,24]

growing and shrinking behavior. Consequently, the research on MT regulation has to focus on understanding how the chemical gradient translates into structural changes that are recognized by these endogenous regulators.

It is known that tubulin has structural plasticity, which is associated with changes in the chemical state and the environment. Noteworthy, there are options to exert a pharmacological control on all of these changes. The first structural transition described in tubulin is related to the association state. Unassembled tubulin is in a "curved" conformation (Figure 1A), irrespective of the nucleotide-bound state.[9] Importantly, the "curved" conformation is also present in oligomeric aggregates[10] and at the MT tips.[11] Meanwhile, in MTs[4] and in $Zn^{2+}$-induced polymers,[12] tubulin is in a "straight" conformation (Figure 1A). The curved-to-straight conformational transition is associated with the formation of lateral contacts between tubulin molecules and can be pharmacologically blocked through two of the drug-binding sites: (i) colchicine[13]—the main alkaloid of the flowering plant *Colchicum autumnale*—and (ii) gatorbulin[2]—a cyclic depsipeptide from marine cyanobacteria. The second conformational change is related to the MT lattice and found in early reports that revealed how MTs assembled from guanosine 5′-[(α,β)methylene]triphosphate (GMPCPP), a slowly hydrolyzable GTP analogue. This induced a helical repeat slightly longer than that found in MTs assembled from GTP, indicating that GMPCPP-tubulin dimers are expanded compared to GDP-bound ones.[14] Because GMPCPP-tubulin is considered a GTP-like bound state, the active form of tubulin has been related to an "expanded" conformation (Figure 1B). However, since guanosine 5′-[(α,β)methylene]diphosphate (GMPCP)-bound tubulin (a GDP-like bound state) is likewise "expanded",[5] it is now clear that expansion is independent of γ-phosphate tubulin activation. Very likely, in these cases, MT lattice expansion is related to the presence of a methylene link between the β- and γ-phosphates. Importantly, this conformational change can be induced by drugs binding to the taxane site, e.g., paclitaxel.[5,14] Finally, a local conformational transition involving loop T5 denotes the presence of GTP or GDP at the nucleotide-binding site. The loop is in an "out" conformation in the presence of GTP (active tubulin) and in an "in" conformation in the presence of GDP[9] (Figure 1C). Otherwise, different phosphate ($AlF_4^-$, $BeF_3^-$) and nucleotide analogues can perfectly mimic this conformational transition,[5] and taxane-site binders can force the transition toward the "out" active conformation.[15]

In addition to these conformational changes, structural plasticity is also evident at the lateral interfaces between


https://doi.org/10.1021/acsomega.2c06926
ACS Omega 2023, 8, 3540−3550

protofilaments. In solution, MTs have certain flexibility to accommodate different numbers of protofilaments, though the most common assembly includes 13 protofilaments (Figure 1D). Interestingly, different nucleotide analogues modulate this number, which can be easily increased or decreased,[5,14] and both taxane-site[16] and laulimalide-site MSAs[17] affect lateral contacts between protofilaments and shift the MT structure toward thicker or thinner filaments as well. Importantly, this shift will directly affect the twist of each protofilament in the MT lattice. In conclusion, the chemical state at the nucleotide-binding site modifies the structure of tubulin and subsequently the MT lattice, changing structural signals recognized by MAPs. In addition, drug modulation directly affects the structure of tubulin and MTs, thus highlighting how the pharmacological regulation can have important consequences on the signaling.

Although "knowing the structure is a way to understand function" (Max Perutz), the structural studies available only provide individual frames taken from the full movie of the functioning of macromolecular complexes. In fact, the study of tubulin and MTs is a continuous challenge from the structural point of view because of tubulin's essential flexibility (crystals can be obtained only in the presence of partner proteins that block tubulin interfaces), MT size (they grow over lengths of several microns), and variability in nature (there exist clear chemical and structural differences associated with the nucleotide-bound state). Therefore, the interpretation of how chemical changes in the tubulin subunits translate into the observed tubulin structure and thereafter into the structural changes described in the MT cap remains controversial.

Macromolecular X-ray crystallography has provided high-resolution structures of tubulin bound to GTP, GDP, and different nucleotide and phosphate analogues (GMPCPP, 5′-[(β,γ)methylene]triphosphate (GMPPCP), GDP·$BeF_3^-$, and GDP·$AlF_4^-$)[5,9] and a broad range of tubulin-modulating drugs.[1,2,18] However, for obtaining the full movie of how these structural changes occur during MT growth and understanding their relationship with the different MAP binding patterns, structural biology must beat the nonuniform and dynamic nature of MTs. Classical structural studies require homogeneous samples to compensate for the low signal provided by individual molecules with the redundancy from perfectly organized molecules,[19] and hence the highly variable structure of the cap is not well suited for this kind of approach. Alternatively, models able to mimic different chemical states have been used to infer the structure of the cap.[5,6,14] These models rely on three types of ligand or protein modifications that result in structurally homogeneous MTs: (1) nucleotide analogues, such as the nonhydrolyzable GMPPCP and guanosine 5′-*O*-[γ-thio] triphosphate (GTP-γS) or the slowly hydrolyzable GMPCPP, which have been developed as structural analogues of the GTP and the GDP·$P_i$ intermediate states;[5,14] (2) phosphate analogues, such as $BeF_3^-$ and $AlF_4^-$, which can bind to the empty γ-phosphate site in GDP-bound tubulin molecules and are considered good analogues of both GTP and GDP·$P_i$;[5] and (3) catalytically defective mutants of tubulin that provide GTP-bound structures.[6] Thus, cryo-electron microscopy (cryo-EM) has yielded structures of MTs in different nucleotide-bound states and in the presence of different drugs or MAPs.[14,20−22] Finally, the combination of these approaches has resulted in different models (yet controversial) of the MT maturation process in which MTs undergo different phases of expanded and compressed forms as well as changes on the protofilament twist. Besides, lateral contacts seem to be less variable, although the lower resolution at these interfaces points to higher flexibility. The main fact is that the cap comprises different lattices that are selectively recognized by MAPs.[7,8]

Not being (yet) able to solve the problem with high-resolution structural approaches, this mini-review focuses on the insight obtained in the regulation of MT function using other complementary methods, in particular: (1) fiber diffraction, as a technique that allows us to follow—in real time—the main MT structural features at both the axial ("expanded" vs "compact") and lateral (number of protofilaments and microtubule diameter) interfaces. Therefore, this method allows us to study the structural response of MTs to drugs and physical changes, and (2) computational approaches that can also provide insight on the time-resolved aspects of the structural modulation process. Finally, tubulin is a family of proteins that spread among eukaryotes, prokaryotes, and viruses. Certainly, most of the tubulin homologues are evolutionarily distinct enough to assemble into filaments far different from MTs. However, BtubA/B from horizontal gene transfer in bacteria[23] and the recently discovered Odin tubulin[24] are structurally close enough to be used as simplified models and to get further insight into the implication of GTPase activity in the formation and dynamics of MTs.

## TIME-RESOLVED RESPONSE OF MTS TO CHEMICAL AND PHYSICAL CHANGES: STUDYING THE CAP WITH FIBER DIFFRACTION

Fiber diffraction is one of the most classical techniques to investigate the structure of biological filaments in physiological conditions without fixation, crystallization, or freezing. Often the sample of interest is natively or artificially arranged on a line of filamentous structures with some regularity, periodicity, or helical pattern (e.g., polypeptide α-helices[26] and muscle fibers[27]). The equipment used for data acquisition and signal analysis is the same as that used by small/wide angle X-ray scattering techniques (SAXS/WAXS). However, while SAXS/WAXS allows us to investigate the shape dynamics of proteins dispersed in buffer solution, fiber diffraction provides more detailed structural information on longitudinal periodicity and lateral spacing of molecules in an arranged filament. Importantly, there are several issues that need to be solved before this technique can be applied to investigate MT structures. The first is to align the filaments in solution, which is not trivial and has been approached in three ways in the case of MTs: (i) using native aligned MTs (e.g., nerve axons[28]); (ii) applying mechanical ultracentrifugation forces to induce MT alignment;[29] and (iii) employing high magnetic fields to force the required arrangement.[30] Since the mechanical force methods required hours to obtain a complete alignment, these approaches did not allow real-time experiments. However, a major breakthrough came from the use of a simple and classical technique of shear flow, which has a long history with other biological structures (e.g., to align actin and tobacco mosaic virus fibers by squeezing them into capillary tubes or in continuous extension flows). Here, the fluid-dynamic properties of the rigid rods or filaments are considered in a stream of medium with a certain gradient of flow velocity to a given shear.[31,32] In order to apply this technique to MTs, Sugiyama et al. developed a new shearing tool, whereby the MT suspension was placed between two discs separated by a narrow gap of 0.3−0.4 mm, and one of the


https://doi.org/10.1021/acsomega.2c06926
ACS Omega 2023, 8, 3540−3550

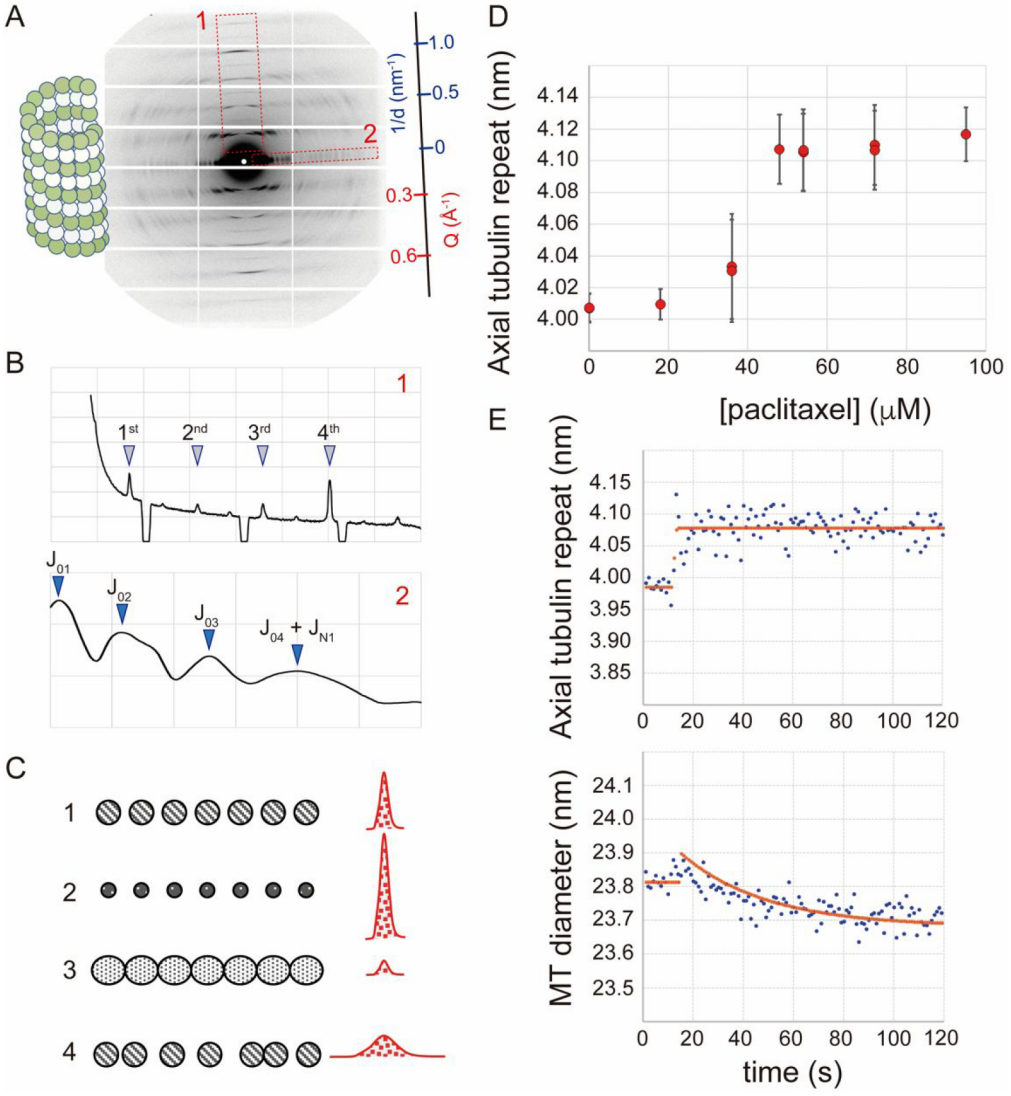


**Figure 2.** X-ray fiber diffraction analysis of MTs. (A) X-ray diffraction pattern from shear-flow aligned MTs. MTs assembled from a purified bovine brain tubulin dimer (43 $\mu$M) at 37 °C with GTP and a total 120 s exposure. From the wedge-shape spreading of equatorial signals, we can estimate the quality of MT orientation, which was not more than 3 degrees. The scale bar indicated both reciprocal spacing [$nm^{-1}$] as well as scattering vector, $Q$-value [$Å^{-1}$], conventionally used for SAXS experiments. (B) Extracted signals along meridional (upper graph) and equatorial (lower graph) axes. (C) Schematic diagram showing how to assume the linear arrangement of unit molecules from the profile data of diffraction. (D) Effect of paclitaxel concentration on the axial repeat of tubulin, corresponding to the mean length of tubulin molecules. Data show a 43 $\mu$M tubulin dimer with 0 to 95 $\mu$M of paclitaxel. Vertical bars indicate the size variation of tubulin estimated from fwhm in the fourth-order diffraction in the meridional axis. (E) Real-time response of preassembled MTs to paclitaxel, where meridional (top) and equatorial (bottom) profiles come from diffraction signals acquired every second. Length change on tubulin axial repeat induced by paclitaxel occurred within 1 s (from 3.98 ± 0.003 nm to 4.08 ± 0.003 nm) with an estimated time constant of 0.16 s. MT diameter seems to decrease with lower rate from 23.8 ± 0.03 nm to 23.7 ± 0.04 nm with an estimated time constant of 34 s, corresponding to rearranging of the protofilament numbers[16] after a small increase of 0.05 nm. Results shown here are from the experiments at the beamline BL40XU (Spring-8, Hygo, Japan, proposal number, 2016B1182, 2019B1365, 2020A1332, 2021A1430).

discs was rotated with a suitable rate, not as high as to fail due to specimen dispersion but high enough to accomplish quick alignment of axonemes isolated from sea urchin spermatozoa. This method enabled us to give a shear rate greater than 1000 $s^{-1}$, $\gamma$; velocity divided the gap; and subsequent modifications allowed us to produce a constant shearing rate in the whole area of the specimen.[32] Importantly, this method: (i) is reasonably cheap in terms of the material needed (a small volume of specimen suspension (<0.1 mL), which for 5−10 mg/mL of tubulin solution implies <1 mg per measurement), (ii) is fast (the wash and exchange of a new sample take less than 1 min, thus allowing for mid-throughput scanning of chemical conditions), and (iii) allows the study of both physical parameters (temperature) and chemicals in real time because the shearing tool is continuously mixing the specimen during continuing data acquisition of diffraction. Besides, radiation damage by the X-ray beam is negligible as the actual volume exposed to the high-intensity beam is less than 2 nL (<0.002% of the total specimen volume).

Figure 2 shows an example of X-ray diffraction signals of GTP-assembled MTs, where four exposures of 30 s (total of 120 s irradiation) were enough to analyze the diffraction signals in the meridional (Figure 2A-1, regular MT axial arrangement) and equatorial (Figure 2A-2, mass of MT in the



https://doi.org/10.1021/acsomega.2c06926
ACS Omega 2023, 8, 3540−3550

diameter direction) axes. The interpretation of the fiber diffractograms is relatively straightforward and provides extremely precise structural data of the MT lattice. The signal profile in the longitudinal direction (Figure 2B) corresponds to a Fourier transform of the periodic arrangement of tubulin molecules, which is a peak of 4 nm ($x$) (corresponding to the size of the tubulin monomer) and additional harmonic patterns that appear as $N \times 1/x$ (where $N$ is an integer called $N^{th}$-order diffraction). The difference in intensity of each peak mainly depends on the helical arrangement of tubulin dimers, and often the signal of the fourth-order (ca. 1 nm), which usually shows the highest intensity on the meridional axis, is used to estimate the length of the tubulin molecules. Notice that the precision in the determination of the mean tubulin length in the example of Figure 2 is less than 0.01 Å, which is much smaller than the wavelength used to record the data and the atom size. This is because the position of the peaks in the meridional axis purely depends on the signal-to-noise ratio of the measured peaks rather than on the wavelength of the X-ray used. Importantly, the intensities (height) of the signals provide information about the density of the structural regularity and the population of aligned molecules (Figure 2C). Therefore, this can be used to follow MT assembly and disassembly (i.e., quick fading of the 1 nm peak during medium cooling or GTP consumption). In addition, the shape of the signals and peak width (full-width at half-maximum, fwhm) can be used to show the magnitude of the regularity of tubulin arrangement in MTs. For instance, the increased randomness of the arrangement of molecules produces decreased intensity and widening of peaks (schematically shown in Figure 2C-4), which is also typical upon paclitaxel binding. Therefore, assuming the semicrystalline structure of MTs with the regularly stacked molecules of tubulin, X-ray diffraction becomes a powerful tool to detect fine but significant structural shifts occurring in tubulin after the binding of specific chemicals or depending on the intermediate state of GTP hydrolysis.[5,32]

In contrast, the equatorial profile (Figure 2B-2) shows a scattering profile that is similar to that observed in molecules with random orientation in solution. In the case of a rod-shape structure, the main scattering can be described as a zero-order Bessel function, which contains mainly four peaks reflecting the diameter. The first strong peak of scattering ($J_{01}$) is obscured and superimposed with background beam noise coming from the shear-flow device window materials, but the second ($J_{02}$) and third ($J_{03}$) peaks can be used to estimate the mean diameter of MTs. The peak signals at scattering angles larger than the fourth peak ($J_{04}$) contain additional signals reflecting the number of protofilament in MTs that can be used to estimate the distribution of MTs with difference protofilament numbers. For example, GDP-MT bound to paclitaxel and GDP-MT bound to the phosphate analogue $BeF_3^-$ have a lower number of protofilaments than GDP-MT bound to the phosphate analogue $AlF_x$ or GMPCPP-MT.[5]

The flexibility of MTs depends on temperature, as initially observed using optical and electron microscopes, where the curvature of the filaments changed in response to thermal fluctuations.[33] In this study, measurements on MT's curvatures gave information on the persistence length of these filaments, which is a parameter that shows their strength. With fiber diffraction, modifications on the flexibility of MTs can be detected as changes of fwhm in the meridional signals[32] in a quick, efficient, and accurate way. For instance, such changes have been described upon paclitaxel binding, with a clear dose dependency (Figure 2D). At low ratios of paclitaxel to tubulin, the diffraction signals of tubulin axial repeat were observed to be dispersed within a small range <0.01 nm (very small fwhm), while the dispersion increased around five times (far higher fwhm) after the MTs were saturated with paclitaxel.

However, most important is the ability for structural time-course measurements provided by fiber diffraction, which allow us to follow real-time changes in response to changes in the sample environment. In this type of experiments, the use of an X-ray beam with high intensity ($10^{14}$ to $10^{15}$ photons/s) is critical since this is the only way to provide accurate signals in short periods of time. For instance, paclitaxel binding (a chemical change) induces a fast change (1 s) in tubulin axial repeat (Figure 2E, top) and a slower change (tens of seconds) on the mean diameter (Figure 2E, bottom, as previously described[16]). Definitely, the use of an X-ray beam with higher flux along with further improvement of tools for X-ray detection are expected to yield more detailed information on structural features and dynamics of MTs.

## MODELING THE MOTIONS: STUDYING THE CAP WITH COMPUTATIONAL METHODS

Computational modeling is another complementary approach that can be used to study the response of tubulin molecules to chemical changes and bound partners. It is particularly instructive to study the dynamic and elastic properties of tubulin using the atomic models of dimers, dimers of dimers, individual protofilaments (or pairs of them), sheets, and microtubular lattices that have been built with the aid of information provided by X-ray diffraction, electron crystallography, and cryo-EM. To this end, normal-mode analysis (NMA) with simplified atomic potentials is an appealing tool because it has been implemented in several user-friendly public servers (e.g., elNémo[34] and iMODS[35]). The elastic network that is created by connecting only the C$\alpha$ atoms (as is usually done) allows the generation of results in terms of simple vibrational motions that are readily calculated and visually understood. In NMA, the distances separating all atom pairs between neighboring monomers that are within a certain cutoff value define the intermonomer "springs" that are treated equivalently in the potential energy function. The harmonic oscillations about the initial configuration that are obtained can reveal important mechanical properties of tubulin, such as persistence lengths, torsional waves, bending stiffness, and other modes of motion that characterize these polymeric structures. Nonetheless, since this type of analysis has been shown to be highly sensitive to the orientation of key loops and subdomains,[36] it is crucially important to avoid the presence of sequence gaps and to accurately model suboptimally optimized regions, e.g., the M-loop, before carrying out the analyses.

NMA has been employed to study both the mechanics of individual intertubulin contact regions[37] and the global mechanical properties of MTs.[38] Thus, the deformation patterns of a 13-protofilament MT (~320 nm long) containing 40 tubulin heterodimers per protofilament (i.e., 520 dimers in total) revealed explicit structural regions (predominantly located at $\alpha\beta$-tubulin interfaces) that undergo both high compression and extension. Three principal patterns of vibrations were identified, namely, axial bending, radial torsion, and longitudinal stretching, the latter apparently connected with deformations in lateral contacts, albeit the mean deformation was about three times smaller than that computed


https://doi.org/10.1021/acsomega.2c06926
ACS Omega 2023, 8, 3540−3550

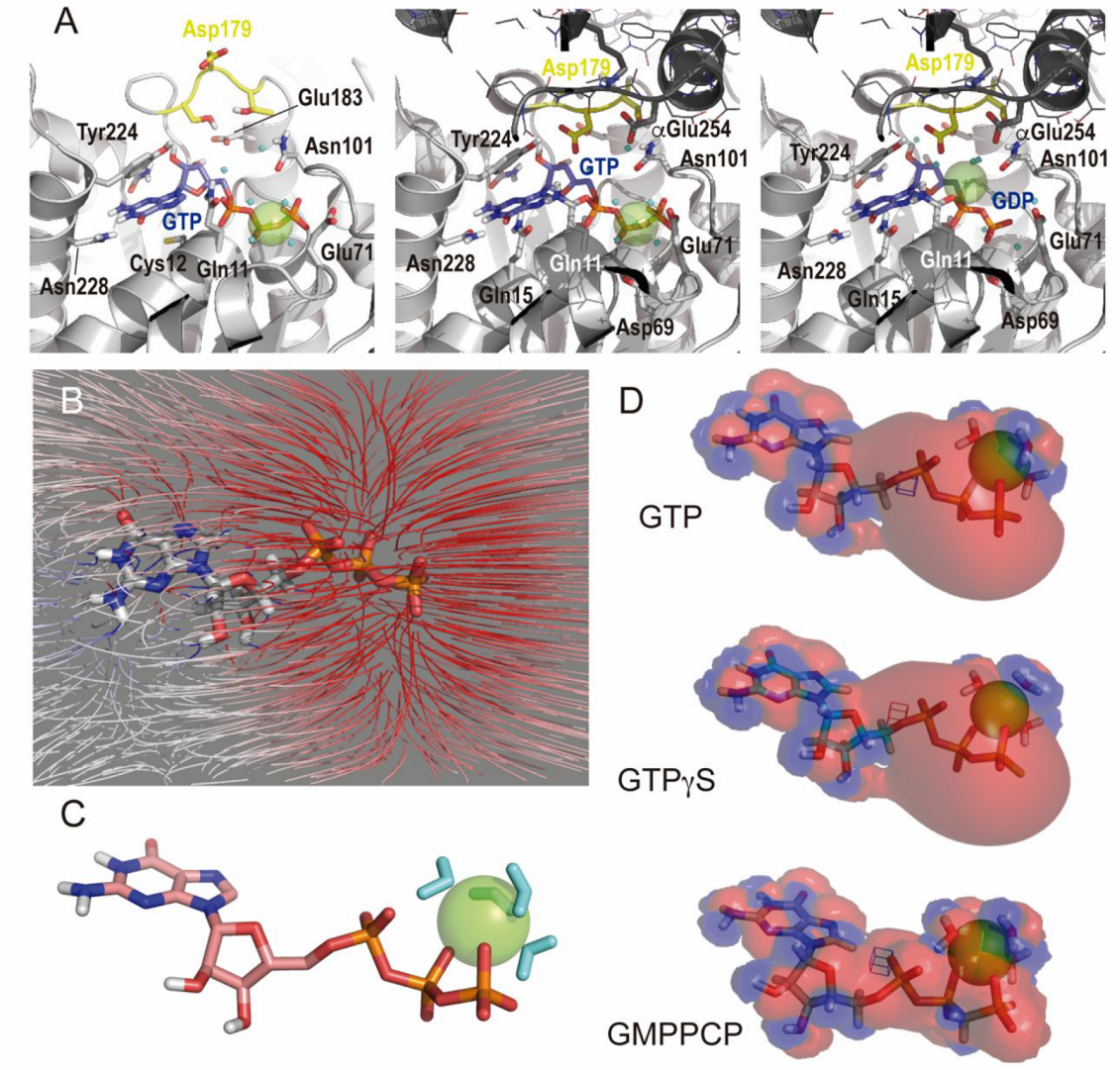


**Figure 3.** Structural and electrostatic differences between GTP and nonhydrolyzable analogues GTP-γS and GMPPCP. (A) Evolution of the nucleotide-bound E-site geometry in a β-tubulin subunit upon polymerization into MTs: the GTP-bound conformation in the presence of a partially solvated $Mg^{2+}$ ion (left) is altered by (i) rearrangement of the $^{178}$Ser-Asp-Thr$^{180}$ switch region in loop T5 (C atoms colored in yellow) upon longitudinal binding of an α-tubulin unit from the next incoming tubulin dimer (middle) and (ii) further catalytic site optimization to trigger water-mediated hydrolysis of the terminal ester bond and produce GDP, which remains bound at the site (right), and $P_i$, which will eventually pass onto the bulk solvent. The polar hydrogens displayed have been reoriented to optimize their H-bonding potential, and water oxygens are shown as small spheres. (B) The electrostatic field lines of GTP (positive and negative polarities in blue and red colors, respectively) indicate the directions of the electrostatic forces surrounding the free nucleotide in solution. (C) Stick model of a GTP molecule bound to a partially desolvated $Mg^{2+}$ ion (green sphere, with water molecules in cyan). (D) The molecular electrostatic potential isosurfaces contoured at ±2 kT/e units (blue and red, respectively) for GTP (top) and nucleotide analogues GTP-γS (middle) and GMPPCP (bottom) highlight regions of hydrogen bond donor/acceptor capabilities in the low dielectric interior of the protein. Atom-centered charges were calculated on the optimized geometries using a 6-31G* basis set, the B3LYP density functional tight-binding (DFTB) method, and the IEF-SCRF continuum solvent model to account for water effects. The APBS program (https://server.poissonboltzmann.org/) was used for the continuum electrostatics calculations, and the results were displayed in PyMOL (v. 1.8.2. Schrodinger LLC) with the aid of an *ad hoc* plugin (https://pymolwiki.org/index.php/APBS).

for bending and torsional modes.[38] Visualization of these motions helps understand the interplay between longitudinal stretching, radial twisting, protofilament number, and minimization of lateral mismatches at the MT seam after GTP hydrolysis. This interplay gives rise to the stochastic fluctuations in the geometry of MT walls and the distinct MT subpopulations recently revealed by a high-resolution cryo-EM refinement method.[39]

A more detailed description of motion can be achieved by means of molecular dynamics (MD) simulations, which have been employed using both coarse-grained[40] and fully atomistic[41] tubulin representations. All-atom MD simulations have consistently predicted curved shapes for both GTP-tubulin and GDP-tubulin,[42−44] and some of them have suggested that (i) most of the energy resulting from GTP hydrolysis is stored in the lattice in the form of longitudinal strain[45] and (ii) the heights of the energy barriers between protofilament conformations govern MT growth and shrinkage.[46] A word of caution is, however, necessary as the results produced by these methods are heavily dependent on the initial configuration of the system so that special attention must be paid to several modeling subtleties such as side chain


https://doi.org/10.1021/acsomega.2c06926
ACS Omega 2023, 8, 3540−3550

rotameric, correct protonation of titratable amino acids, and a proper octahedral arrangement of binding motifs for the nucleotide-bound, partially desolvated $Mg^{2+}$ ions.[47] In this respect, it has to be noted that densities due to the majority of Asp and Glu side chains are lacking in cryo-EM images of MTs due to their high susceptibility to radiation damage during electron exposure.[48] The problem is compounded by the fact that the $Mg^{2+}$ ion in many crystal structures may accidentally wander off into the water positions during refinement if the resolution is not high enough.[49] Thus, any modeling work that uses experimentally solved tubulin structures as templates must aim to ensure that the initial geometries for dual nucleotide and cation binding in both $\alpha$- and $\beta$-tubulin subunits are correct. In addition, from a chemical perspective, it should be borne in mind that the slowly hydrolyzable analogues GMPCPP and GTP$\gamma$S, which have been so successfully employed as valuable mimics of GTP in recent cryo-EM work on MTs,[14,22,39,48] have hydrogen bonding potentials different from those of GTP itself, and this may subtly affect the torsion angles of the phosphate tail in the solvated polar environment of the nucleotide-binding site at the $\beta-\alpha$ interface. In fact, a suboptimal binding geometry of GMPCPP is likely to be responsible for the originally reported 4- to 8-fold lower affinity for tubulin relative to GTP and for the extremely slow hydrolysis rate of its $\beta-\gamma$ bond when incorporated into the MT lattice.[50] Moreover, control experiments have supported the view that lattice expansion in GMPPCP- and GMPCP-MTs is due to the presence of the methylene group linking $\alpha$- and $\beta$-phosphates rather than the $\gamma$-phosphate in the GTP mimic GMPPCP.[5]

When GTP and GDP binding sites in $\alpha$- and $\beta$-tubulin are inspected in a high-resolution crystal structure, e.g., the epothilone-bound $T_2R-TTL$ complex (composed of two head-to-tail bound $\alpha\beta$-tubulin heterodimers plus the stathmin-like protein RB3 plus a tubulin tyrosine ligase fragment),[51] it becomes apparent that both the location and coordination spheres of the bound $Mg^{2+}$ ions differ (Figure 3B). Thus, although both cations have four bound water molecules from the first hydration shell, the $Mg^{2+}$ ion at the GTP-binding site is coordinated to O1$\beta$ and O1$\gamma$ phosphate oxygens, whereas that at the GDP-binding site is coordinated by O1$\alpha$ and the side-chain carbonyl of Gln11, a residue that can also hydrogen-bond to $\beta$Gln247 but not to $\alpha$Ala247. Interestingly, recent cryo-EM work has provided evidence to support the view that wild-type GDP-MTs and GTP$\gamma$S-MTs display a compacted lattice,[48] whereas GMPCPP-MTs[40,48] and MTs containing E254A and E254N $\alpha$-tubulin variants[6] have expanded (or uncompressed) lattices instead. Thus, it seems reasonable to assume that these changes are likely to be promoted by the distinct electrostatic interactions between the side-chain carboxylate of $\alpha$Glu254 (in helix H8) and the phosphate-bound, partially hydrated $Mg^{2+}$ ion at the nucleotide-binding site in $\beta$-tubulin. As a result, the interdimer longitudinal interface in the MT is strengthened upon GTP hydrolysis.[48]

Since the preferred mechanism for GTP hydrolysis at the exchangeable site (E-site) in $\beta$-tubulin is a solvent-assisted pathway[52] that involves the rate-limiting nucleophilic attack of a properly oriented water molecule onto the $\gamma$-phosphorus atom, subtle changes in geometry—particularly of the $\gamma$-phosphate and the side-chain carboxylate of Glu254 from $\alpha$-tubulin—are likely to have a large impact on the feasibility and rate of GTP hydrolysis. Moreover, the resulting transition state, when achieved, must evolve toward the final products, that is, the $Mg^{2+}$-bound GDP, which remains at the site within the MT lattice, and $H_2PO_4^-$, whose exit is probably facilitated by (i) hydrogen bond rupture and reformation, (ii) proton transfers, (iii) conformational changes in the protein, and (iv) enhanced solvation.[53] In accordance with this reasoning, it is conceivable that the proper arrangement for GTP hydrolysis at the nucleotide-binding site in $\beta$-tubulin during maturation of the GTP cap is contingent on additional protein motions and further side-chain reorientations that are necessary for deep entrance of the catalytic $\alpha$Glu254 carboxylate and subsequent water activation. In this regard, it is highly informative that recent high-resolution X-ray crystal structures of tubulin dimers solved in the presence of $\gamma$-phosphate analogues ($BeF_3^-$ or $AlF^-_4/AlF_3$) have revealed a conformational toggle switch involving $^{178}$Ser-Asp-Thr$^{180}$ in loop T5 (between S5 and H5) of $\beta$-tubulin[5] that is likely to be triggered by binding of another tubulin dimer to the growing MT tip; this sequence stretch is strictly conserved in all $\beta$-tubulin isotypes and differs from the corresponding $^{178}$Ser-Thr-Ala$^{180}$ in $\alpha$-tubulin. The backbone carbonyl of Asp179 hydrogen bonds to the amino group of the incoming $\alpha$Lys352 which, in turn, hydrogen bonds to the $\alpha$Glu254 carboxylate that is crucial for catalysis. The distinct mechanistic possibilities that couple phosphate cleavage, proton transfer, and phosphate release in $\beta$-tubulin upon polymerization can be explored by using the same hybrid methods that combine quantum mechanics with classical molecular mechanics (QM/MM) and have been so successfully employed to clarify various enzymatic mechanisms.[53] It will be imperative to characterize the reorganization of the electrostatic environment around the terminal phosphate groups as well as the precise pH-dependent protonation state of the terminal $\gamma$-phosphate over the MT maturation process to properly account for the hydrolytic mechanism.[54] This chemical view is in accordance with the evidence that (i) paclitaxel-induced expansion likely happens after GTP hydrolysis and (ii) the presence of $\gamma$-phosphate analogues ($BeF_3^-$ or $AlF^-_4/AlF_3$) reverts paclitaxel-induced expansion.[5]

## SIMPLIFYING THE SYSTEM: LESSONS FROM PROKARYOTES

A usual way to gain insight into the functioning of complex biological systems is to identify and examine a comparable but simpler and more easily interpretable model. Tubulins are a family of proteins spread over eukaryotes, prokaryotes, and viruses. Two members of the family, bacterial (Btub, of *Prostecobacter* species[55]) and Odin (in the Asgard archaea[24]) tubulins (Figure 1E), are very close structural homologues to the eukaryotic one. In fact, both are proposed to have evolved from a primitive eukaryotic cell by horizontal gene transfer.[23,24] These proteins have the typical domain architecture of the family and also typical $\alpha,\beta$-tubulin features like the extension of the loops and the two large helices that face the wall of the MT (involved in the interaction with many MAPs). However, they also display some key differences that make them an ideal simplified version of their eukaryotic counterpart. Odin tubulin is a single monomer that displays an active catalytic loop (similar to $\alpha$-tubulin) and a short S9−S10 loop in the taxane site (similar to $\beta$-tubulin). Btubs are two proteins, BtubA and BtubB, that form a transient heterodimer and also include an active catalytic loop and a short S9−S10 loop in each of them. As mentioned, the association into linear polymers is mandatory for the completion of the catalytic site and the activation of GTPase activity (this is common in the tubulin


https://doi.org/10.1021/acsomega.2c06926
ACS Omega 2023, 8, 3540−3550

superfamily of proteins), and hydrolysis contributes to the dynamics of the assembled filaments. Therefore, the presence of an active catalytic loop is a hallmark of tubulins, and the existence of an inactive loop in $\beta$-tubulin (due to the replacement of Glu with Lys) is an exception that likely evolved to allow the formation of more complex polymers. Meanwhile, the presence of a shorter S9−S10 loop in $\beta$-tubulin defines the taxane site, which is a well-known pharmacological regulatory site in tubulin and mediates MT stabilization. Importantly, Btubs and Odin tubulin lack the characteristic acidic C-terminal tail of $\alpha$- and $\beta$-tubulins.

High-resolution structures of Odin tubulin included a crystal-packing-related protofilament[24] and showed that, as previously described for eukaryotic tubulin[25] and FtsZ,[56] the GTPase activating switch involves the complementation of the GTP-binding pocket of the lower subunit in the protofilament with two water-polarizing residues that are in direct contact with the attacking water molecule for $\gamma$-phosphate hydrolysis. In contrast, the Odin tubulin showed a $Na^+$ ion coordinating the water-polarizing residues with the $\gamma$-phosphate, apart from the typical $Mg^{2+}$ ion coordinated by two nucleotide phosphate oxygens. Otherwise, the activation mechanism of GTP hydrolysis among tubulins is highly conserved. Remarkably, structural comparison of GTP-bound Odin tubulin and its apo- and GDP-bound counterparts suggested that GTP hydrolysis involves an upward movement of the central H7 helix together with loops H6−H7 and T7 and the entire intermediate domain, similar to the conformational change described in $\alpha$-tubulin.[14] In addition, changes at the N-terminal domain include the downward movement of the H1−S2 loop and the shift of the T5 loop into an "in" conformation (as initially described in the curved conformation of GDP-tubulin[9]). These movements would correspond to an axial compaction upon GTP hydrolysis. However, the extent to which these changes affect the protofilament structure is difficult to assess due to crystal packing. Noteworthy, in Odin tubulin's structure, the M-loop is perfectly ordered into a helix, as shown for $\alpha\beta$-tubulin, which could allow the formation of lateral contacts between molecules similar to those made by tubulin in MTs.

Odin tubulin in solution is able to polymerize in the absence of $Mg^{2+}$ (no other tubulin protein has shown this behavior before). This assembly involves the formation of salt-induced irregular bundles with a not well-defined internal structure,[24] and whether or not GTP hydrolysis occurs in this kind of filament has not been analyzed yet. Moreover, in the presence of $Mg^{2+}$, the protein switches to the formation of filaments that closely resemble the tight, one-start helical ones formed by GDP-tubulin (i.e., stacked washer-like[57]). Notice that in $\alpha\beta$-tubulin the C-terminal tail contributes to the formation of the filament and induces distinct bending at the intradimer and interdimer interfaces. However, since Odin tubulin lacks the C-terminal acidic tail of tubulin and is a monomeric protein, the same bending is expected between consecutive molecules, and this could be related to the looser appearance of the resulting tubes. Finally, the orientation of the monomer in the protofilaments of these tubes is similar to that of eukaryotic GDP-tubulin rings, and hence, lateral contacts mediated by the M-loop are not expected in these $Mg^{2+}$-induced Odin tubulin filaments either.

BtubA and BtubB polymerize through the formation of a heterodimer, BtubAB, which assembles into a 4-protofilament mini-MT that does not differ much from a mammalian-MT, except for its size.[58] The different biochemical properties of eukaryotic $\alpha\beta$-tubulin (a stable heterodimer building block) and BtubAB (two building blocks that interact with each other upon assembly) might have an implication on the growth into the resulting filament structure. In addition, differences at the loops involved in the formation of lateral contacts likely contribute to the modification of the interprotofilament angle, which is 90° in BtubAB and 27.7° in eukaryotic 13-protofilament MTs.[58] In BtubAB mini-MTs, GTP hydrolysis takes places in all subunits (as revealed in the cryo-EM structure showing that all subunits contain GDP[58]). This difference could be related to the formation of a more compact lattice in those mini-MTs, which have a rise of 79.3 Å versus that of 81.5 Å in GDP-MTs.[14] Furthermore, this structure highlighted that BtubA and BtubB also undergo a curved-to-straight conformational transition due to the formation of lateral contacts, which similarly to tubulin rely exclusively on the loop-mediated latch model (with Tyr-283 in the M-loop of one subunit acting as the rotating bolt and H1-S2/H2-S3 of the lateral partner acting as the stationary keeper). However, the key interacting residue in tubulin, Tyr283, is replaced by Phe287 in BtubA (similar to yeast tubulin[59]) and Gln281 in BtubB, and in mini-MTs only the M-loop of BtubA establishes both homotypic (A−A) and heterotypic (A−B) lateral interactions, whereas the M-loop of BtubB is not ordered. Consequently, the lattice is likely to be more labile than that of eukaryotic MTs. Alternatively, given that it is difficult to assess specific interactions involving the M-loop at the resolution of these cryo-EM structures, it is plausible that the mini-MT structure has captured an intermediate pre-depolymerization state. Loss of lateral interactions in one of the subunits while keeping them in the other point to a singular and sequential mechanism of depolymerization could explain: (i) the rapid depolymerization during dynamic instability and (ii) the high plasticity found in MT lattices, which are able to gain or lose protofilaments very quickly.[16] Remarkably, mini-MTs can also follow dynamic instability and treadmilling,[58] denoting the presence of a GTP cap similar to that in $\alpha,\beta$-tubulin MTs. Considering this, structural information on mini MTs in different nucleotide-bound states could shed light on the effect of GTP and GTP hydrolysis on the filament structure. Indeed, MTs show different protofilament twists depending on the nucleotide content,[5] which could differentially affect homotypic and heterotypic lateral contacts. It still remains to be found whether the mini-MT lattice expands as the MT does in the presence of certain nucleotide analogues (GMPCPP and GMPCP,[5,14] drugs bound at the taxane site,[14,20] and amino acid replacements at the $\alpha$-tubulin catalytic loop)[6] or as do others found in non-mammalian sources (where the protofilament number is also somewhat smaller[59,60]).

From these prokariotic examples we learned that the typical tubulin fold of two main domains split by a central helix provides the scaffold for the formation of axial contacts (protofilaments) and GTP hydrolysis. However, the formation of lateral contacts does not follow a strict rule because the presence of the M-loop does not ensure the assembly into a hollow cylinder (as happens in the assembly of Odin tubulin). Instead, the duplication into two different molecules able to copolymerize seems to be an essential step toward the formation of MTs. In MTs, the nucleotide-binding site is occluded, and there is no nucleotide exchange in the polymer, which makes the GTP cap a key structure on the maintenance of the filament and responsible for filament dynamics.


https://doi.org/10.1021/acsomega.2c06926
ACS Omega 2023, 8, 3540−3550

## CONCLUDING REMARKS

In this mini-review we described three alternative methods to obtain information on MT-cap morphology and structure that can improve our current understanding of MT function. First, we presented how combining the classical but well-established theory of diffraction with updated detecting tools and the shear-flow aligning technique makes it is possible to turn the X-ray fiber diffraction of MTs in a powerful method to get insights into precise (<0.001 nm) and dynamic (<1 s) structural information under various physical and chemical conditions. With this quick and reliable technique, it would be possible to perform structural screening of the effects of specific MSA on MTs, allowing the design of structurally tailored MT stabilizers, which combined with cell biology studies will help us to understand the structural tubulin code and its cellular effects. Second, we show how simplified elastic network models of several tubulin assemblies shed light on the range and directions of prevalent motions that control subunit interactions as well as lateral and longitudinal angle variations in MTs. Hybrid QM/MM methods, in turn, are likely to help us answer the question of how the chemical environment around the terminal phosphate of GTP evolves over MT maturation to trigger water-mediated hydrolysis. Finally, we have seen how the prokaryotic world provides supporting information on the functioning of tubulins and the implication of GTP hydrolysis in filament dynamics.

## AUTHOR INFORMATION


### Corresponding Author

**J. Fernando Díaz** − *Unidad de Desarrollo de Fármacos Biológicos, Inmunológicos y Químicos, Centro de Investigaciones Biológicas Margarita Salas - Consejo Superior de Investigaciones Científicas, E-28040 Madrid, Spain;* orcid.org/0000-0003-2743-3319; Email: fer@cib.csic.es

### Authors

**María Ángela Oliva** − *Unidad de Desarrollo de Fármacos Biológicos, Inmunológicos y Químicos, Centro de Investigaciones Biológicas Margarita Salas - Consejo Superior de Investigaciones Científicas, E-28040 Madrid, Spain;* orcid.org/0000-0002-2215-4639

**Federico Gago** − *Department of Biomedical Sciences and IQM-UAH Associate Unit, University of Alcalá, E-28805 Alcalá de Henares, Spain;* orcid.org/0000-0002-3071-4878

**Shinji Kamimura** − *Department of Biological Sciences, Faculty of Science and Engineering, Chuo University, 112-8551 Tokyo, Japan*

Complete contact information is available at: https://pubs.acs.org/10.1021/acsomega.2c06926


### Notes

The authors declare no competing financial interest.

### Biographies

María A. Oliva studied Biology and gained her Ph.D. in Biochemistry and Molecular Biology studying the bacterial cell division protein FtsZ at Complutense University, Madrid. She followed postdoctoral structural studies at the MRC-Laboratory of Molecular Biology, Cambridge, with an EMBO Long-Term Fellowship, under the supervision of Dr. Jan Löwe. Since 2012 she has lead the research line of the "Tubulin family of proteins activation and regulation mechanisms" at Centro de Investigaciones Biologicas of the Spanish Research Council. She focuses on understanding the activation switch of tubulins and their pharmacological regulation, with the ultimate goal of translating this information to control the related biological processes. She exploits the opportunity offered by a multidisciplinary approach combining biochemistry, biophysics, and structural studies. Dr. Oliva is a member of the Spanish Societies of Biophysics, Biochemistry and Molecular Biology and Synchrotron Users Association. She is a Life Science chair at ALBA Synchrotron (Barcelona) and has been part of the teacher board at Universidad Internacional Menendez Pelayo, Madrid, contributing to the Summer School and the Molecular and Cellular Integrative Biology Master Degree.

Federico Gago studied Pharmacy at Complutense University, Madrid, postdoctoral studies at the Physical Chemistry Laboratory, Oxford University, under the supervision of Prof. W. Graham Richards. He teaches Pharmacology at the School of Pharmacy and the School of Medicine in the University of Alcalá, near Madrid, where he is a Full Professor of Pharmacology in the Department of Biomedical Sciences. He was Associate Director of the NFCR Center for Computational Drug Design (Oxford) from 2001 to 2006 and a member of the Editorial Advisory Board of *Journal of Medicinal Chemistry* from 2006 to 2010. Since 2001 he has been serving as an Editor-in-Chief for *Journal of Computer-Aided Molecular Design*. Prof. Gago is a member of the Spanish Societies of Medicinal Chemistry, Biochemistry and Molecular Biology, Biophysics, and Pharmacology as well as of the Spanish Association for Cancer Research. He has authored more than 200 research papers in specialized scientific journals and published several reviews and book chapters. His current research interests are in the areas of catalytic mechanisms in enzymes, receptor-based structure−activity relationships, structure-based drug design, and computer simulations of drug-targeted macromolecules including DNA, enzymes, and pharmacological receptors.

Shinji Kamimura received his received his B.S. in Zoology from Faculty of Science, The University of Tokyo, Tokyo, Japan. He then received his M.S. and Ph.D. in Animal Physiology from Faculty of Science, The University of Tokyo, Tokyo, Japan. During his master and doctor courses, his main research topics were on the activity analysis of velocity and generated forces of sliding microtubules in flagellar axonemes. He continued the research works in the same field of cell motility as a postdoctoral (Bioholonics Project, ERATO, Japan) and an assistant (the University of Tokyo, Tokyo, Japan). His main work was on the nanometer-precision analysis of high-frequency vibration (~8 nm in amplitude) observed in activated axonemes under a conventional optical microscope. To understand more details of the activity of native axonemes and microtubules in a scale of atoms, he started to use improved techniques of X-ray fiber diffraction at the synchrotrons of KEK (with K. Wakabayashi) and SPring-8 (with H. Iwamoto) in Japan. His present main interest is how the structure of native microtubules changes depending on chemical and physical conditions.

J. Fernando Díaz has focused his research on the natural and pharmacological mechanisms of modulation of protein switches. He received his degree in Chemistry from Universidad Complutense de Madrid in 1988. In 1989 he joined Centro de Investigaciones Biológicas Margarita Salas (Madrid, Spain), under the direction of Prof. José Manuel Andreu, to work on his Master Thesis focused on the molecular mechanisms of action of colchicine. In 1993 he presented at Universidad Complutense de Madrid his Ph.D. thesis developed between Centro de Investigaciones Biológicas Margarita Salas and Daresbury Laboratory (Daresbury, UK), studying the mechanisms of tubulin activation by taxol. From 1994 until 1999 he was assistant researcher at Katholieke Universiteit Leuven (Belgium)



https://doi.org/10.1021/acsomega.2c06926
ACS Omega 2023, 8, 3540−3550

working in the mechanisms of ras-p21 activation. He returned to Centro de Investigaciones Biológicas Margarita Salas as a tenure track scientist to investigate the bacterial tubulin analogue FtsZ. Since 2001, he has been a tenured scientist and leader of the "Structure, function and pharmacology of cytoskeleton research" group. Among his major findings is the description of three novel regulatory sites in tubulin, Laulimalide/Peloruside, Maytansine, and Gatorbuline. From 2021 he is head of the "Unit for development of Biological, Immunological and Chemical drugs" of Centro de Investigaciones Biológicas Margarita Salas.

## ■ ACKNOWLEDGMENTS

This work was supported by Spanish Ministerio de Ciencia e Innovación PID2021-123399OB-I00, PID2019-104545RBI00/AEI/10.13039/501100011033 and and PID2019-104070RB-C22 to M.O.B., J.F.D. and F.G., respectively; Consejo Superior de Investigaciones Científicas PIE 201920E111; the European Commission-NextGenerationsEU (Regulation EU 2020/2094, through CSIC's Global Health Platform (PTI Salud Global)); and Proyecto de Investigación en Neurociencia Fundación Tatiana Pérez de Guzmán el Bueno 2020 to J.F.D.; and Grant-in-Aid for Exploratory Research (#20657014) and Grants-in-Aid for Scientific Research on Priority Areas (#17H03668, #19K06602) from MEXT, Japan, to S.K.

## ■ REFERENCES

(1) Steinmetz, M. O.; Prota, A. E. Microtubule-Targeting Agents: Strategies To Hijack the Cytoskeleton. *Trends Cell Biol.* **2018**, *28* (10), 776−792.
(2) Matthew, S.; Chen, Q.-Y.; Ratnayake, R.; Fermaintt, C. S.; Lucena-Agell, D.; Bonato, F.; Prota, A. E.; Lim, S. T.; Wang, X.; Díaz, J. F.; Risinger, A. L.; Paul, V. J.; Oliva, M. A.; Luesch, H. Gatorbulin-1, a distinct cyclodepsipeptide chemotype, targets a seventh tubulin pharmacological site. *Proc. Natl. Acad. Sci. U.S.A.* **2021**, *118* (9), No. e2021847118.
(3) Mühlethaler, T.; Milanos, L.; Ortega, J. A.; Blum, T. B.; Gioia, D.; Roy, B.; Prota, A. E.; Cavalli, A.; Steinmetz, M. O. Rational Design of a Novel Tubulin Inhibitor with a Unique Mechanism of Action. *Angew. Chem., Int. Ed. Engl.* **2022**, *61* (25), No. e202204052.
(4) Nogales, E.; Whittaker, M.; Milligan, R. A.; Downing, K. H. High-resolution model of the microtubule. *Cell* **1999**, *96* (1), 79−88.
(5) Estevez-Gallego, J.; Josa-Prado, F.; Ku, S.; Buey, R. M.; Balaguer, F. A.; Prota, A. E.; Lucena-Agell, D.; Kamma-Lorger, C.; Yagi, T.; Iwamoto, H.; Duchesne, L.; Barasoain, I.; Steinmetz, M. O.; Chretien, D.; Kamimura, S.; Diaz, J. F.; Oliva, M. A. Structural model for differential cap maturation at growing microtubule ends. *Elife* **2020**, DOI: 10.7554/eLife.50155.
(6) LaFrance, B. J.; Roostalu, J.; Henkin, G.; Greber, B. J.; Zhang, R.; Normanno, D.; McCollum, C. O.; Surrey, T.; Nogales, E. Structural transitions in the GTP cap visualized by cryo-electron microscopy of catalytically inactive microtubules. *Proc. Natl. Acad. Sci. U. S. A.* **2022**, *119* (2), No. e2114994119.
(7) Akhmanova, A.; Steinmetz, M. O. Microtubule + TIPs at a glance. *J. Cell Sci.* **2010**, *123* (20), 3415−9.
(8) Akhmanova, A.; Steinmetz, M. O. Microtubule minus-end regulation at a glance. *J. Cell Sci.* **2019**, DOI: 10.1242/jcs.227850.
(9) Nawrotek, A.; Knossow, M.; Gigant, B. The determinants that govern microtubule assembly from the atomic structure of GTP-tubulin. *J. Mol. Biol.* **2011**, *412* (1), 35−42.
(10) Diaz, J. F.; Pantos, E.; Bordas, J.; Andreu, J. M. Solution structure of GDP-tubulin double rings to 3 nm resolution and comparison with microtubules. *J. Mol. Biol.* **1994**, *238* (2), 214−25.
(11) Chretien, D.; Fuller, S. D.; Karsenti, E. Structure of growing microtubule ends: two-dimensional sheets close into tubes at variable rates. *J. Cell Biol.* **1995**, *129* (5), 1311−28.
(12) Nogales, E.; Wolf, S. G.; Downing, K. H. Structure of the alpha beta tubulin dimer by electron crystallography. *Nature* **1998**, *391* (6663), 199−203.
(13) Ravelli, R. B.; Gigant, B.; Curmi, P. A.; Jourdain, I.; Lachkar, S.; Sobel, A.; Knossow, M. Insight into Tubulin Regulation from a Complex with Colchicine and a Stathmin-like Domain. *Nature* **2004**, *428* (6979), 198−202.
(14) Alushin, G. M.; Lander, G. C.; Kellogg, E. H.; Zhang, R.; Baker, D.; Nogales, E. High-Resolution Microtubule Structures Reveal the Structural Transitions in $\alpha\beta$-Tubulin upon GTP Hydrolysis. *Cell* **2014**, *157* (5), 1117−1129.
(15) Balaguer, F. A.; Muhlethaler, T.; Estevez-Gallego, J.; Calvo, E.; Gimenez-Abian, J. F.; Risinger, A. L.; Sorensen, E. J.; Vanderwal, C. D.; Altmann, K. H.; Mooberry, S. L.; Steinmetz, M. O.; Oliva, M. A.; Prota, A. E.; Diaz, J. F. Crystal Structure of the Cyclostreptin-Tubulin Adduct: Implications for Tubulin Activation by Taxane-Site Ligands. *Int. J. Mol. Sci.* **2019**, *20* (6), 1392.
(16) Díaz, J. F.; Valpuesta, J. M.; Chacón, P.; Diakun, G.; Andreu, J. M. Changes in microtubule protofilament number induced by Taxol binding to an easily accessible site. Internal microtubule dynamics. *J. Biol. Chem.* **1998**, *273* (50), 33803−10.
(17) Estévez-Gallego, J.; Álvarez-Bernad, B.; Pera, B.; Wullschleger, C.; Raes, O.; Menche, D.; Martínez, J. C.; Lucena-Agell, D.; Prota, A. E.; Bonato, F.; Bargsten, K.; Cornelus, J.; Giménez-Abián, J. F.; Northcote, P.; Steinmetz, M. O.; Kamimura, S.; Altmann, K.-H.; Paterson, I.; Gago, F.; Van der Eycken, J.; Díaz, J. F.; Oliva, M. A. Chemical modulation of microtubule structure through the laulimalide/peloruside site. *Structure* **2023**, *31*, 88.
(18) Mühlethaler, T.; Gioia, D.; Prota, A. E.; Sharpe, M. E.; Cavalli, A.; Steinmetz, M. O. Comprehensive Analysis of Binding Sites in Tubulin. *Angew. Chem., Int. Ed.* **2021**, *60* (24), 13331−13342.
(19) Nogales, E.; Scheres, S. H. Cryo-EM: A Unique Tool for the Visualization of Macromolecular Complexity. *Mol. Cell* **2015**, *58* (4), 677−89.
(20) Kellogg, E. H.; Hejab, N. M. A.; Howes, S.; Northcote, P.; Miller, J. H.; Diaz, J. F.; Downing, K. H.; Nogales, E. Insights into the Distinct Mechanisms of Action of Taxane and Non-Taxane Microtubule Stabilizers from Cryo-EM Structures. *J. Mol. Biol.* **2017**, *429* (5), 633−646.
(21) Kellogg, E. H.; Hejab, N. M. A.; Poepsel, S.; Downing, K. H.; DiMaio, F.; Nogales, E. Near-atomic model of microtubule-tau interactions. *Science* **2018**, *360* (6394), 1242−1246.
(22) Zhang, R.; LaFrance, B.; Nogales, E. Separating the effects of nucleotide and EB binding on microtubule structure. *Proc. Natl. Acad. Sci. U.S.A.* **2018**, *115* (27), E6191−E6200.
(23) Schlieper, D.; Oliva, M. A.; Andreu, J. M.; Lowe, J. Structure of bacterial tubulin BtubA/B: Evidence for horizontal gene transfer. *Proc. Natl. Acad. Sci. U. S. A.* **2005**, *102*, 9170.
(24) Akıl, C.; Ali, S.; Tran, L. T.; Gaillard, J.; Li, W.; Hayashida, K.; Hirose, M.; Kato, T.; Oshima, A.; Fujishima, K.; Blanchoin, L.; Narita, A.; Robinson, R. C. Structure and dynamics of Odinarchaeota tubulin and the implications for eukaryotic microtubule evolution. *Science Advances* **2022**, *8* (12), No. eabm2225.
(25) Nogales, E.; Downing, K. H.; Amos, L. A.; Lowe, J. Tubulin and FtsZ form a distinct family of GTPases. *Nat. Struct. Biol.* **1998**, *5* (6), 451−8.
(26) Klug, A.; Crick, F. H. C.; Wyckoff, H. W. Diffraction by helical structures. *Acta Crystallogr.* **1958**, *11* (3), 199−213.
(27) Huxley, H. E.; Brown, W. The low-angle x-ray diagram of vertebrate striated muscle and its behaviour during contraction and rigor. *J. Mol. Biol.* **1967**, *30* (2), 383−434.
(28) Wais-Steider, C.; White, N. S.; Gilbert, D. S.; Eagles, P. A. X-ray diffraction patterns from microtubules and neurofilaments in axoplasm. *J. Mol. Biol.* **1987**, *197* (2), 205−18.
(29) Mandelkow, E.; Thomas, J.; Cohen, C. Microtubule structure at low resolution by x-ray diffraction. *Proc. Natl. Acad. Sci. U. S. A.* **1977**, *74* (8), 3370−4.
(30) Bras, W.; Diakun, G. P.; Díaz, J. F.; Maret, G.; Kramer, H.; Bordas, J.; Medrano, F. J. The Susceptibility of Pure Tubulin to High


https://doi.org/10.1021/acsomega.2c06926
*ACS Omega* 2023, 8, 3540−3550

Magnetic Fields: A Magnetic Birefringence and X-Ray Fiber Diffraction Study. *Biophysical journal* **1998**, *74* (3), 1509−1521.
(31) Sugiyama, T.; Miyashiro, D.; Takao, D.; Iwamoto, H.; Sugimoto, Y.; Wakabayashi, K.; Kamimura, S. *Quick Shear-Flow Alignment of Biological Filaments for X-ray Fiber Diffraction Facilitated by Methylcellulose* **2009**, *97*, 3132−8.
(32) Kamimura, S.; Fujita, Y.; Wada, Y.; Yagi, T.; Iwamoto, H. X-ray fiber diffraction analysis shows dynamic changes in axial tubulin repeats in native microtubules depending on paclitaxel content, temperature and GTP-hydrolysis. *Cytoskeleton* **2016**, *73* (3), 131−144.
(33) Gittes, F.; Mickey, B.; Nettleton, J.; Howard, J. Flexural rigidity of microtubules and actin filaments measured from thermal fluctuations in shape. *J. Cell Biol.* **1993**, *120* (4), 923−34.
(34) Suhre, K.; Sanejouand, y.-h. ElNemo: A Normal Mode Web Server for Protein Movement Analysis and the Generation of Templates for Molecular Replacement. *Nucleic acids research* **2004**, *32*, W610−4.
(35) López-Blanco, J. R.; Aliaga, J. I.; Quintana-Ortí, E. S.; Chacón, P. iMODS: internal coordinates normal mode analysis server. *Nucleic Acids Res.* **2014**, *42*, W271−6.
(36) ben-Avraham, D.; Tirion, M. M. Dynamic and elastic properties of F-actin: a normal-modes analysis. *Biophysical journal* **1995**, *68* (4), 1231−1245.
(37) Molodtsov, M. I.; Grishchuk, E. L.; Efremov, A. K.; McIntosh, J. R.; Ataullakhanov, F. I. Force production by depolymerizing microtubules: A theoretical study. *Proc. Natl. Acad. Sci. U. S. A.* **2005**, *102* (12), 4353−4358.
(38) Havelka, D.; Deriu, M. A.; Cifra, M.; Kučera, O. Deformation pattern in vibrating microtubule: Structural mechanics study based on an atomistic approach. *Sci. Rep.* **2017**, *7* (1), 4227.
(39) Debs, G. E.; Cha, M.; Liu, X.; Huehn, A. R.; Sindelar, C. V. Dynamic and asymmetric fluctuations in the microtubule wall captured by high-resolution cryoelectron microscopy. *Proc. Natl. Acad. Sci. U. S. A.* **2020**, *117* (29), 16976−16984.
(40) Bollinger, J. A.; Imam, Z. I.; Stevens, M. J.; Bachand, G. D. Tubulin islands containing slowly hydrolyzable GTP analogs regulate the mechanism and kinetics of microtubule depolymerization. *Sci. Rep* **2020**, *10* (1), 13661.
(41) Hemmat, M.; Castle, B. T.; Sachs, J. N.; Odde, D. J. Multiscale Computational Modeling of Tubulin-Tubulin Lateral Interaction. *Biophysical journal* **2019**, *117* (7), 1234−1249.
(42) Igaev, M.; Grubmüller, H. Microtubule assembly governed by tubulin allosteric gain in flexibility and lattice induced fit. *eLife* **2018**, *7*, No. e34353.
(43) Fedorov, V. A.; Orekhov, P. S.; Kholina, E. G.; Zhmurov, A. A.; Ataullakhanov, F. I.; Kovalenko, I. B.; Gudimchuk, N. B. Mechanical properties of tubulin intra- and inter-dimer interfaces and their implications for microtubule dynamic instability. *PLOS Computational Biology* **2019**, *15* (8), No. e1007327.
(44) Tong, D.; Voth, G. A. Microtubule Simulations Provide Insight into the Molecular Mechanism Underlying Dynamic Instability. *Biophys. J.* **2020**, *118* (12), 2938−2951.
(45) Igaev, M.; Grubmüller, H. Microtubule instability driven by longitudinal and lateral strain propagation. *PLOS Computational Biology* **2020**, *16* (9), No. e1008132.
(46) Igaev, M.; Grubmüller, H. Bending-torsional elasticity and energetics of the plus-end microtubule tip. *Proc. Natl. Acad. Sci. U.S.A.* **2022**, *119* (12), No. e2115516119.
(47) Yang, Y.; Chakravorty, D. K.; Merz, K. M., Jr. Finding a needle in the haystack: computational modeling of Mg2+ binding in the active site of protein farnesyltransferase. *Biochemistry* **2010**, *49* (44), 9658−66.
(48) Manka, S. W.; Moores, C. A. The role of tubulin-tubulin lattice contacts in the mechanism of microtubule dynamic instability. *Nat. Struct Mol. Biol.* **2018**, *25* (7), 607−615.
(49) Rudack, T.; Jenrich, S.; Brucker, S.; Vetter, I. R.; Gerwert, K.; Kötting, C. Catalysis of GTP hydrolysis by small GTPases at atomic detail by integration of X-ray crystallography, experimental, and theoretical IR spectroscopy. *J. Biol. Chem.* **2015**, *290* (40), 24079−90.
(50) Hyman, A. A.; Salser, S.; Drechsel, D. N.; Unwin, N.; Mitchison, T. J. Role of GTP hydrolysis in microtubule dynamics: information from a slowly hydrolyzable analogue, GMPCPP. *Mol. Biol. Cell* **1992**, *3* (10), 1155−67.
(51) Prota, A. E.; Bargsten, K.; Zurwerra, D.; Field, J. J.; Diaz, J. F.; Altmann, K. H.; Steinmetz, M. O. Molecular mechanism of action of microtubule-stabilizing anticancer agents. *Science* **2013**, *339* (6119), 587−90.
(52) Calixto, A. R.; Moreira, C.; Pabis, A.; Kötting, C.; Gerwert, K.; Rudack, T.; Kamerlin, S. C. L. GTP Hydrolysis Without an Active Site Base: A Unifying Mechanism for Ras and Related GTPases. *J. Am. Chem. Soc.* **2019**, *141* (27), 10684−10701.
(53) Berta, D.; Buigues, P. J.; Badaoui, M.; Rosta, E. Cations in motion: QM/MM studies of the dynamic and electrostatic roles of H + and Mg2+ ions in enzyme reactions. *Curr. Opin. Struct. Biol.* **2020**, *61*, 198−206.
(54) Kamerlin, S. C.; Sharma, P. K.; Prasad, R. B.; Warshel, A. Why nature really chose phosphate. *Q. Rev. Biophys.* **2013**, *46* (1), 1−132.
(55) Jenkins, C.; Samudrala, R.; Anderson, I.; Hedlund, B. P.; Petroni, G.; Michailova, N.; Pinel, N.; Overbeek, R.; Rosati, G.; Staley, J. T. Genes for the cytoskeletal protein tubulin in the bacterial genus Prosthecobacter. *Proc. Natl. Acad. Sci. U. S. A.* **2002**, *99* (26), 17049−54.
(56) Oliva, M. A.; Cordell, S. C.; Lowe, J. Structural insights into FtsZ protofilament formation. *Nat. Struct Mol. Biol.* **2004**, *11* (12), 1243−50.
(57) Wang, H. W.; Nogales, E. Nucleotide-dependent bending flexibility of tubulin regulates microtubule assembly. *Nature* **2005**, *435* (7044), 911−5.
(58) Deng, X.; Fink, G.; Bharat, T. A. M.; He, S.; Kureisaite-Ciziene, D.; Löwe, J. Four-stranded mini microtubules formed by *Prosthecobacter* BtubAB show dynamic instability. *Proc. Natl. Acad. Sci. U. S. A.* **2017**, *114* (29), E5950−E5958.
(59) Howes, S. C.; Geyer, E. A.; LaFrance, B.; Zhang, R.; Kellogg, E. H.; Westermann, S.; Rice, L. M.; Nogales, E. Structural and functional differences between porcine brain and budding yeast microtubules. *Cell Cycle* **2018**, *17* (3), 278−287.
(60) Howes, S. C.; Geyer, E. A.; LaFrance, B.; Zhang, R.; Kellogg, E. H.; Westermann, S.; Rice, L. M.; Nogales, E. Structural differences between yeast and mammalian microtubules revealed by cryo-EM. *J. Cell Biol.* **2017**, *216* (9), 2669−2677.


https://doi.org/10.1021/acsomega.2c06926
*ACS Omega* 2023, 8, 3540−3550